

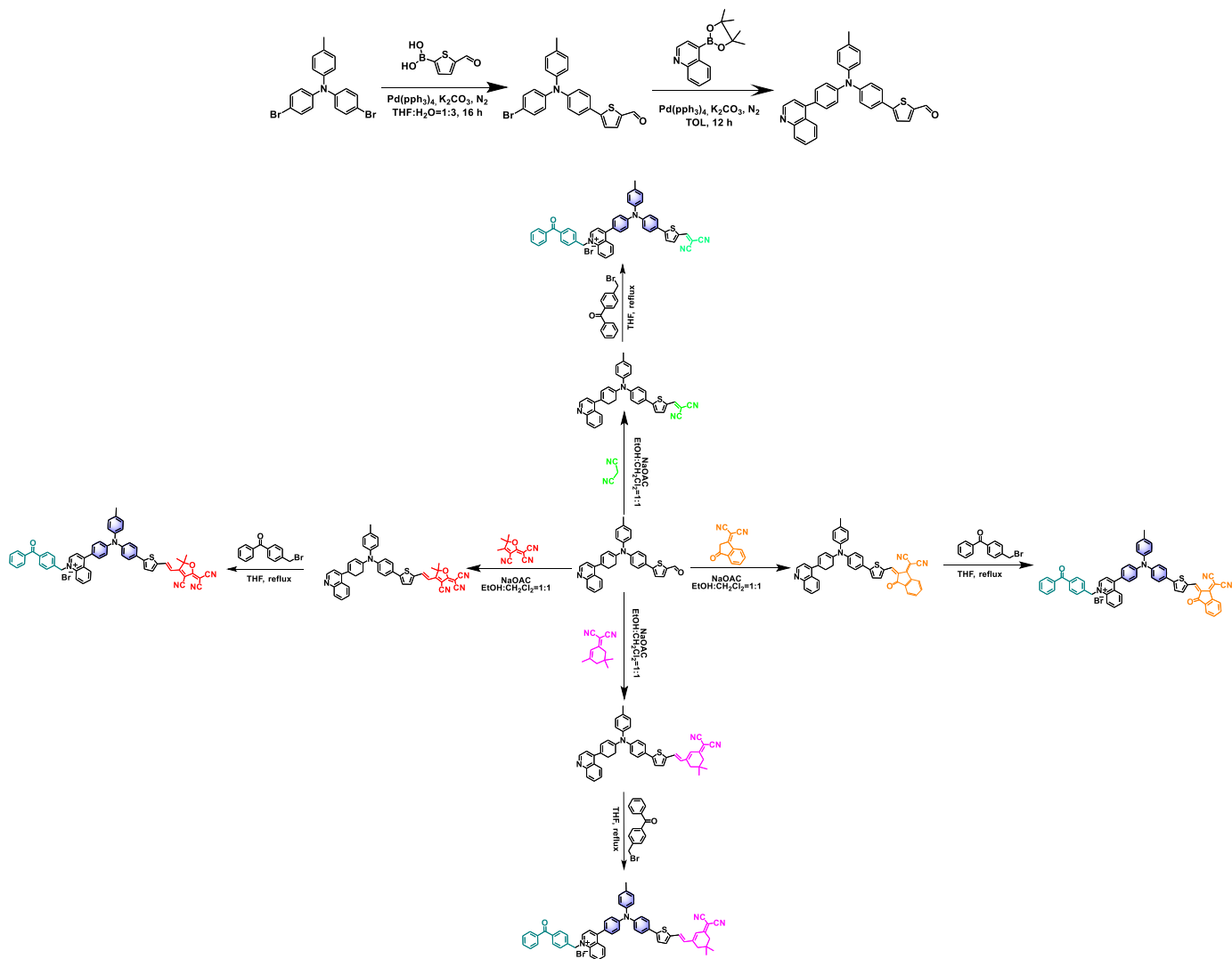
## Supporting Information

### **Phototherapeutic applications of benzophenone-containing NIR-emitting photosensitizers based on different receptor modulations**

Shuge Chen,<sup>a,b</sup> Jianqing Li,<sup>c</sup> Weidong Yin,<sup>b</sup> Weiqiang Li,<sup>b</sup> Xitong He,<sup>b</sup> Hui Liang,<sup>b</sup> Zarfar Mahmood,<sup>b</sup> Yanping Huo,<sup>b</sup> Zujin Zhao,<sup>\*c</sup> and Shaomin Ji<sup>\*a,b</sup>

Guangdong Provincial Laboratory of Chemistry and Fine Chemical Engineering Jieyang Center,  
Jieyang, P. R. China.  
E-mail: smji@gdut.edu.cn

## 1. Synthesis



Scheme S1. Synthetic routes of CN-TPAQ-BP, ICN-TPAQ-BP, FCN-TPAQ-BP and ACN-TPAQ-BP.

## 1. $^1\text{H}$ and $^{13}\text{C}$ NMR spectra

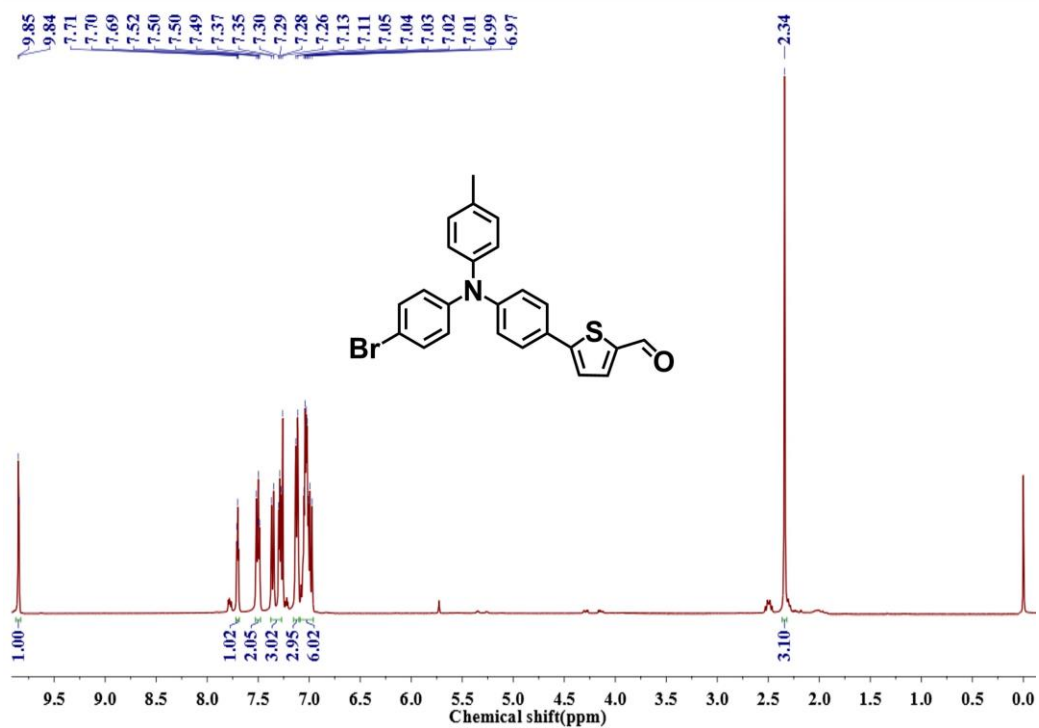


Fig. S1 <sup>1</sup>H NMR spectrum of TPA-T in CDCl<sub>3</sub>.

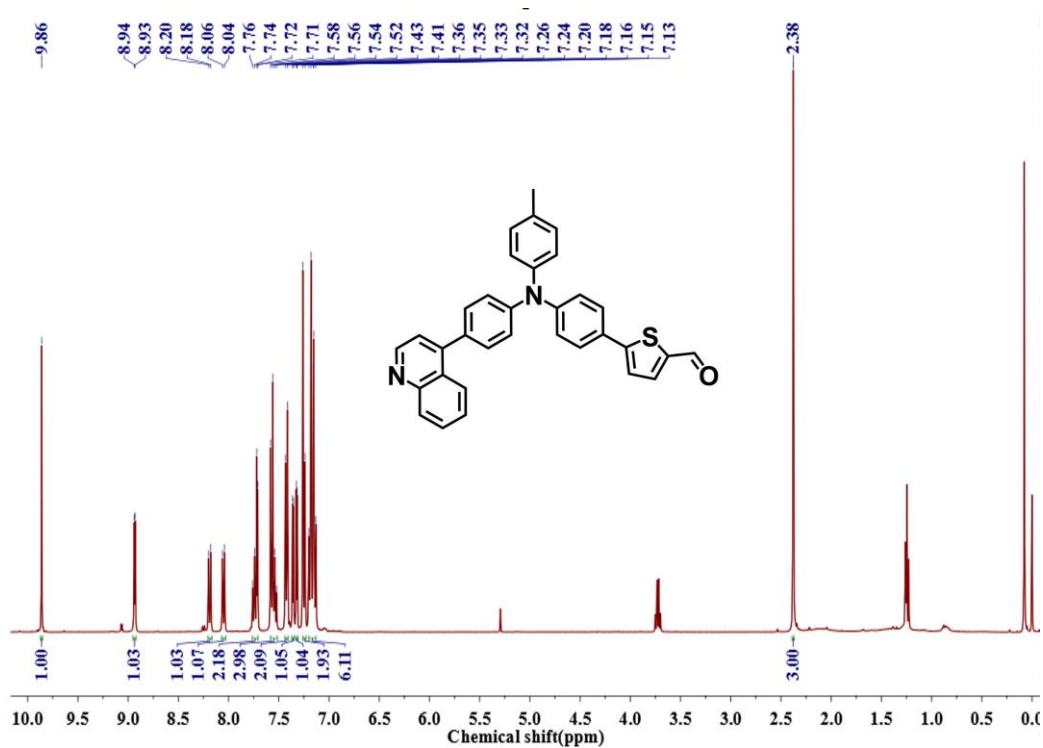


Fig. S2 <sup>1</sup>H NMR spectrum of TPAQ-T in CDCl<sub>3</sub>.

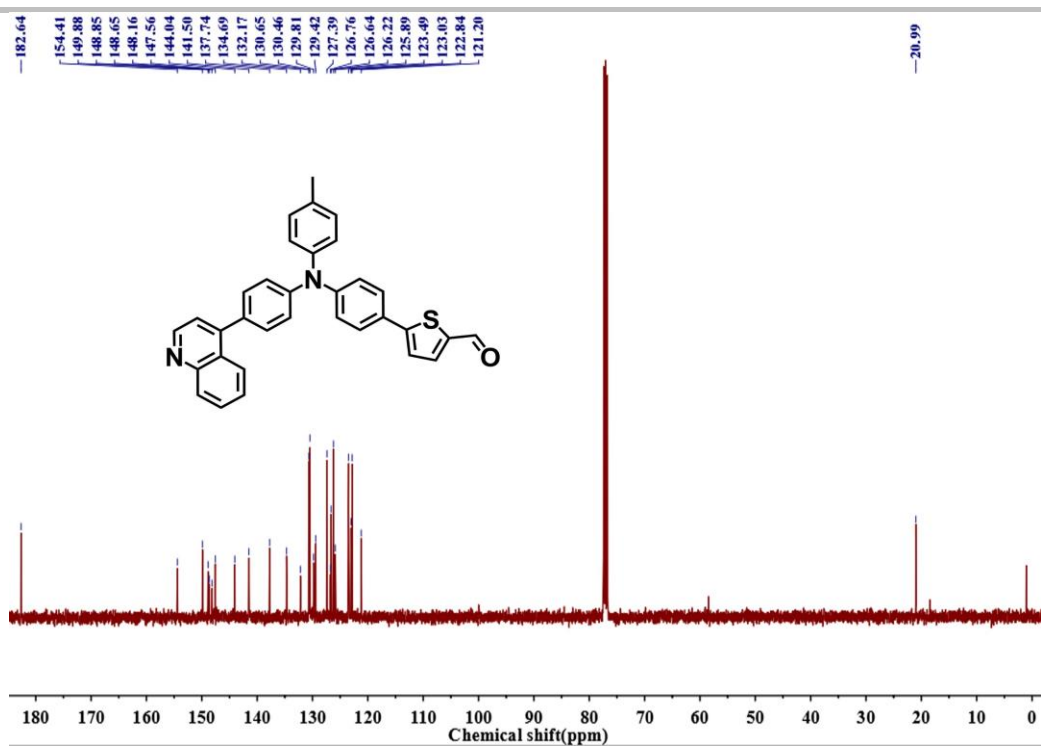


Fig. S3 <sup>13</sup>C NMR spectrum of TPAQ-T in CDCl<sub>3</sub>.

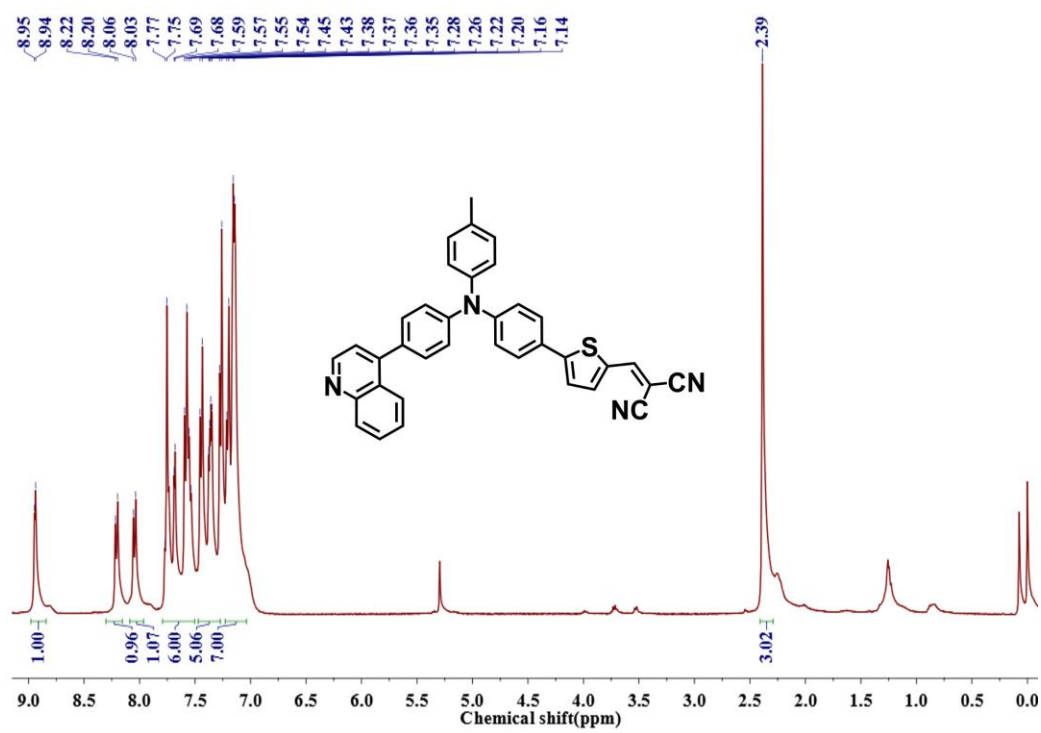


Fig. S4 <sup>1</sup>H NMR spectrum of CN-TPAQ in CDCl<sub>3</sub>.

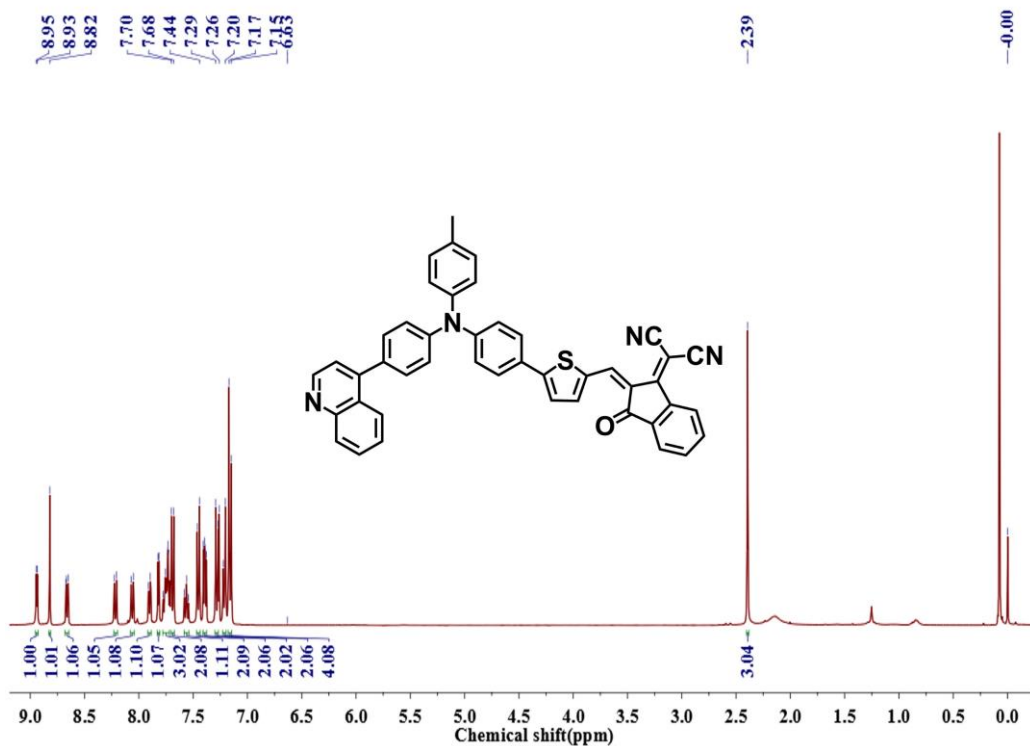


Fig. S5  $^1\text{H}$  NMR spectrum of ICN-TPAQ in  $\text{CDCl}_3$ .

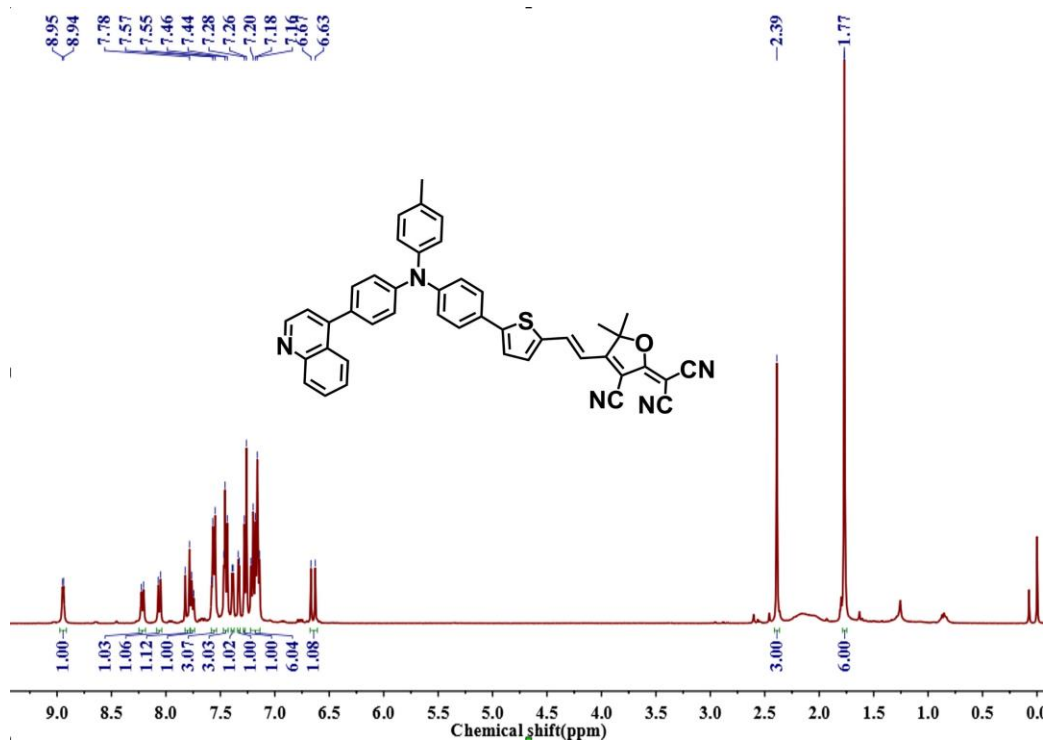


Fig. S6  $^1\text{H}$  NMR spectrum of FCN-TPAQ in  $\text{CDCl}_3$ .

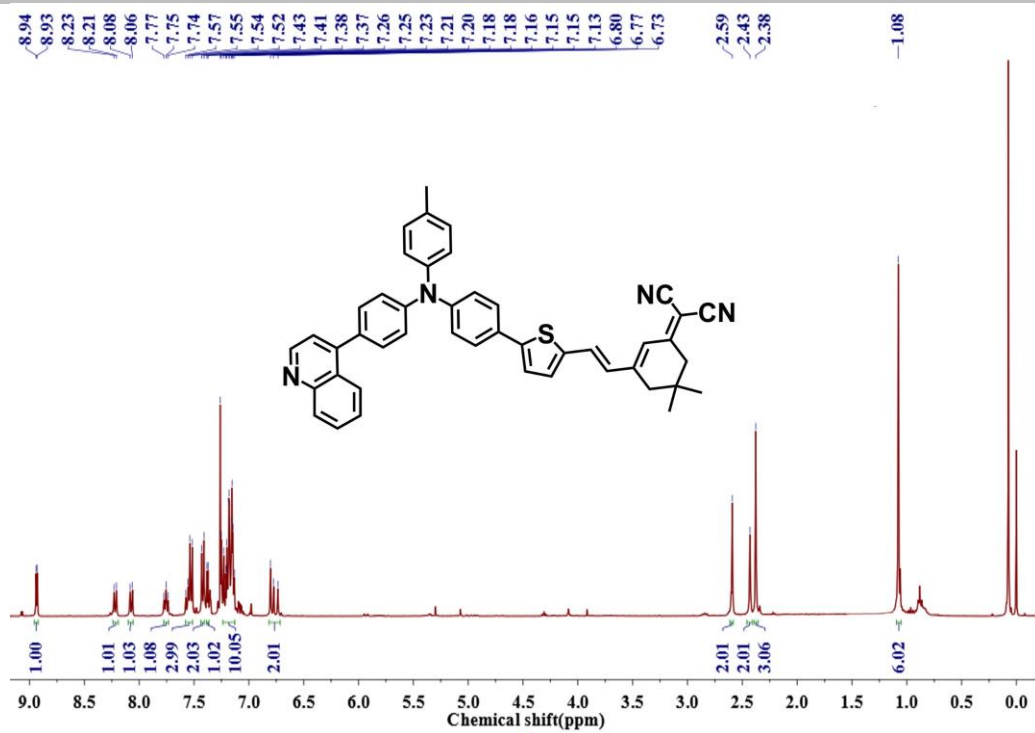


Fig. S7 <sup>1</sup>H NMR spectrum of ACN-TPAQ in CDCl<sub>3</sub>.

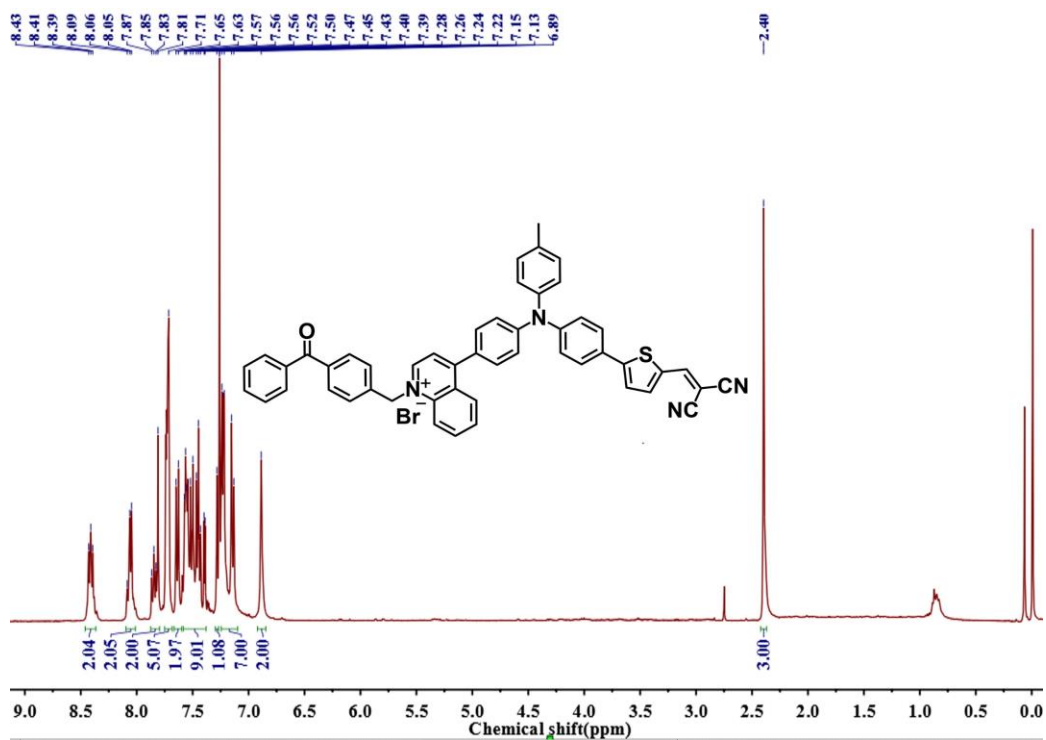


Fig. S8 <sup>1</sup>H NMR spectrum of CN-TPAQ-BP in CDCl<sub>3</sub>.

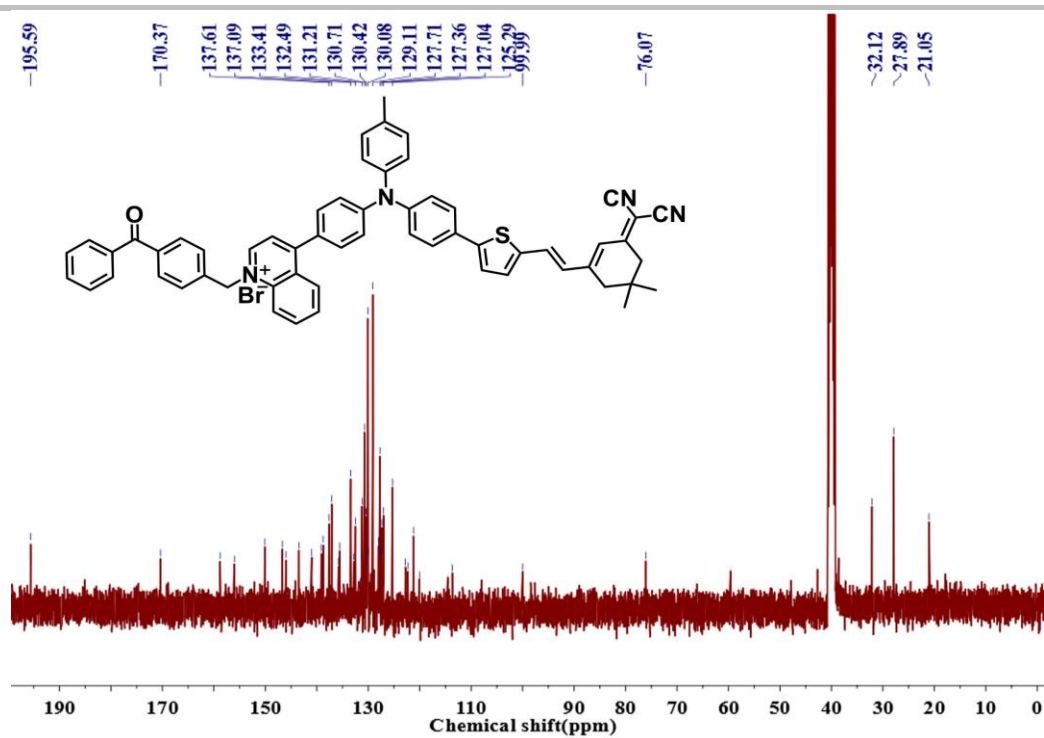


Fig. S9  $^{13}\text{C}$  NMR spectrum of CN-TPAQ-BP in  $\text{CDCl}_3$ .

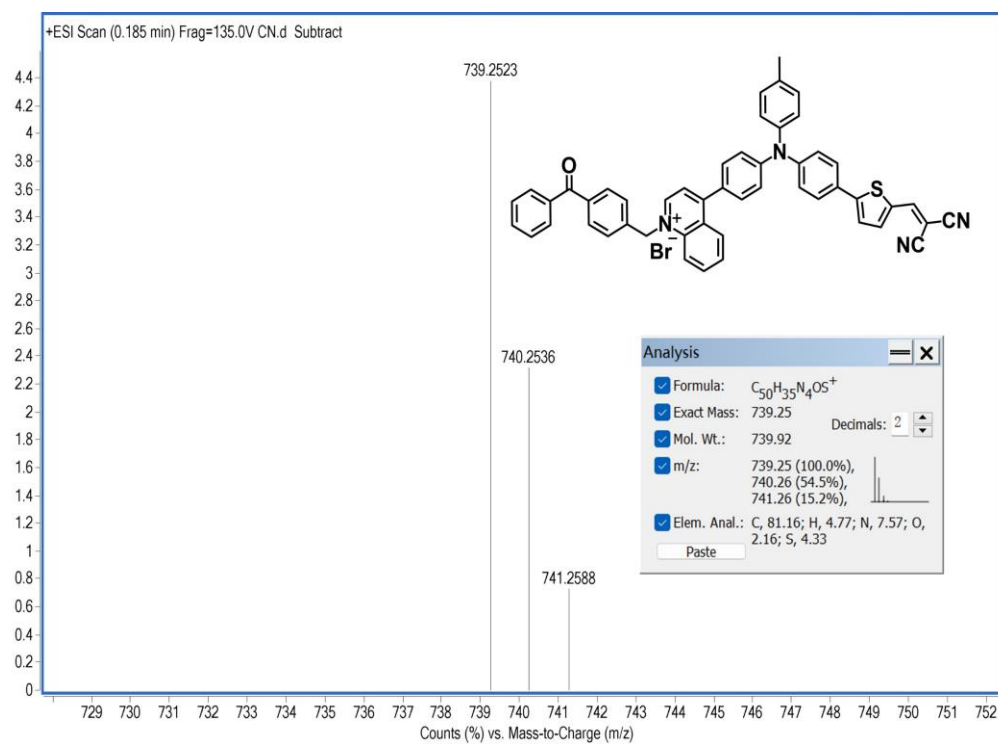


Fig. S10 ESI-MS spectrum of CN-TPAQ-BP.

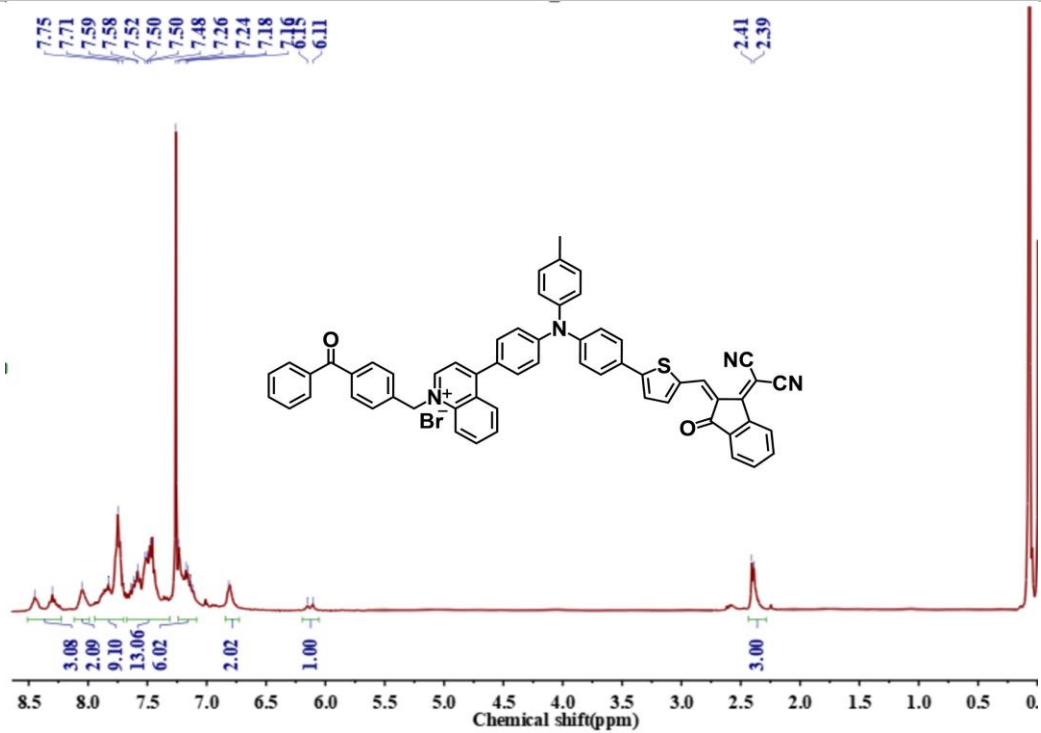


Fig. S11 <sup>1</sup>H NMR spectrum of ICN-TPAQ-BP in CDCl<sub>3</sub>

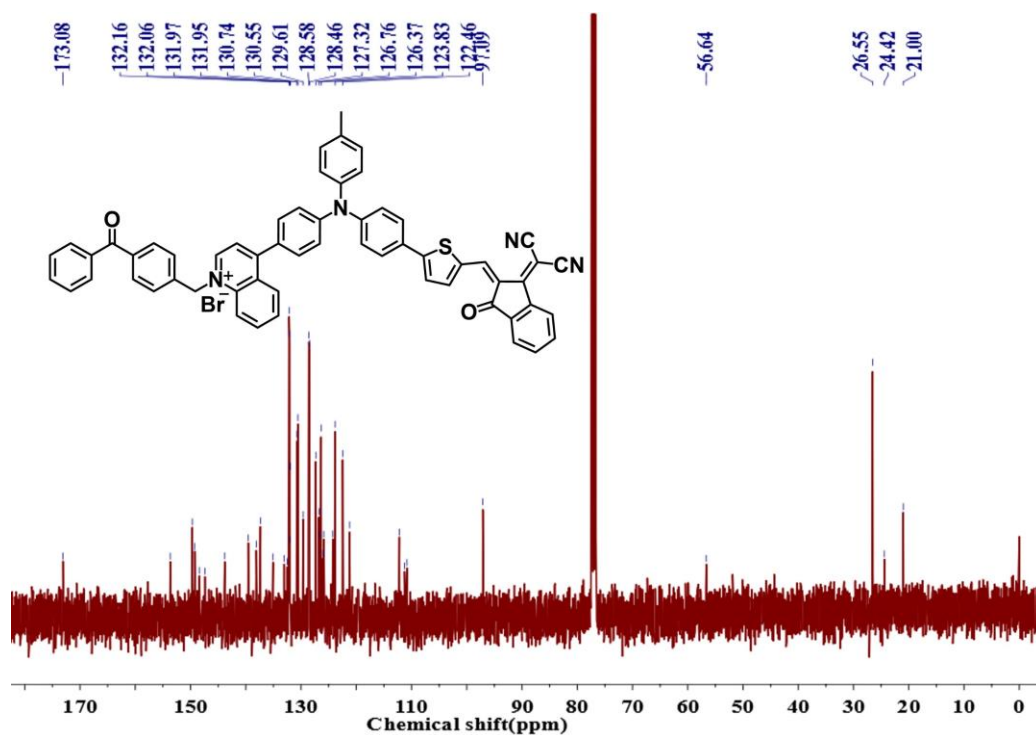


Fig. S12 <sup>13</sup>C NMR spectrum of ICN-TPAQ-BP in CDCl<sub>3</sub>.



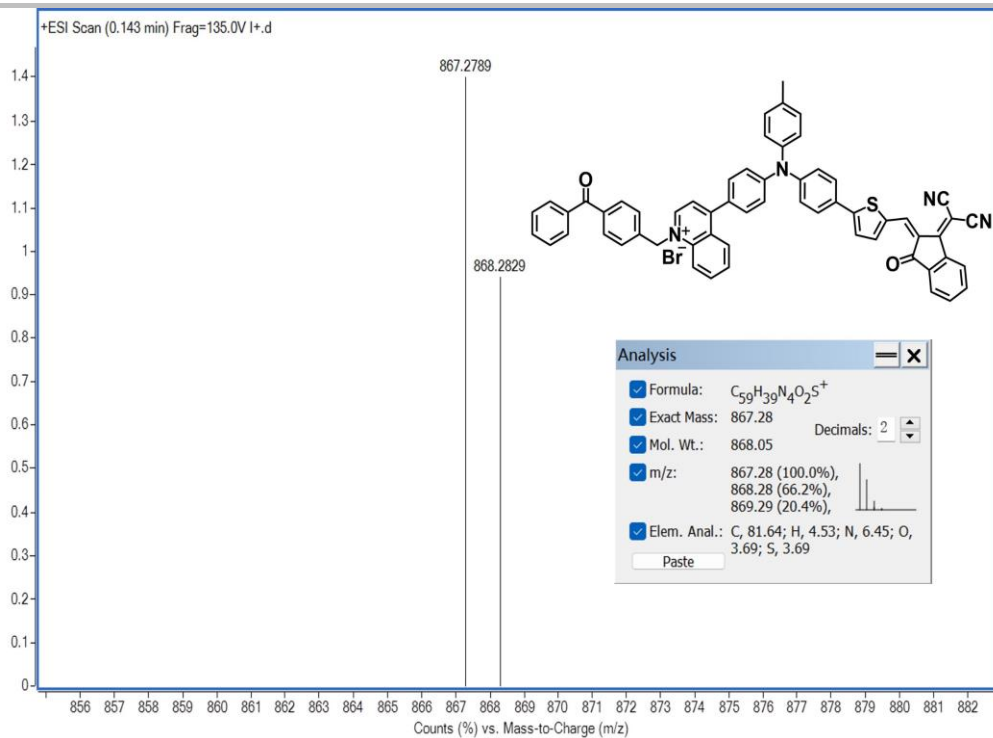


Fig. S13 ESI-MS spectrum of ICN-TPAQ-BP.

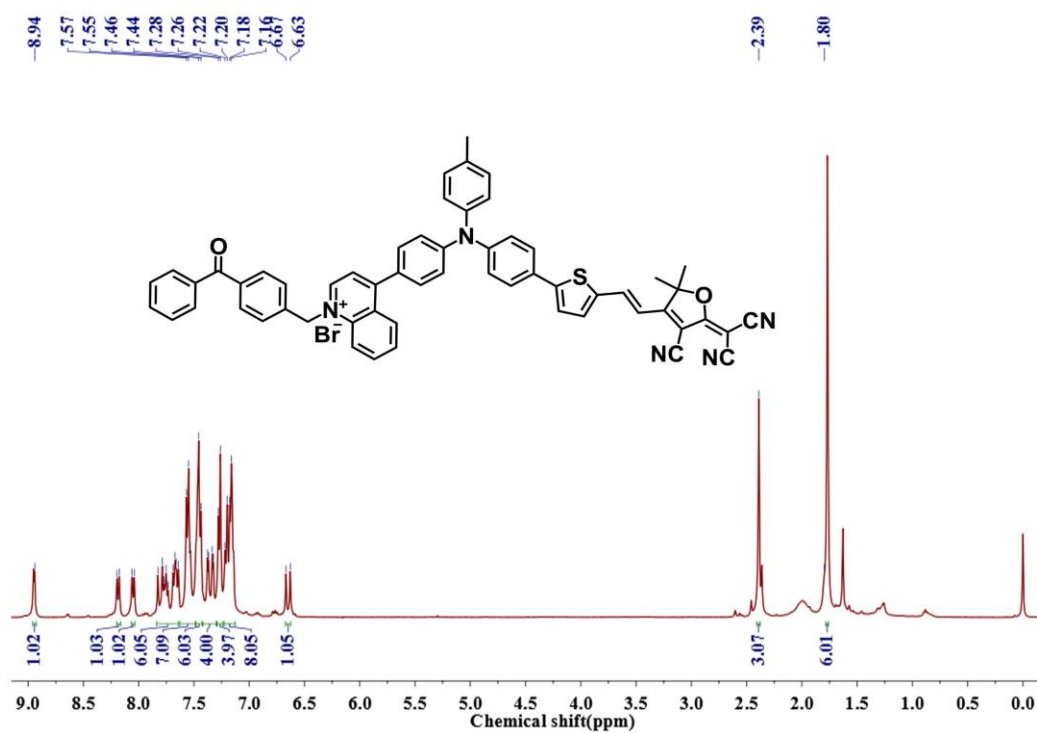


Fig. S14  $^1H$  NMR spectrum of FCN-TPAQ-BP in  $CDCl_3$

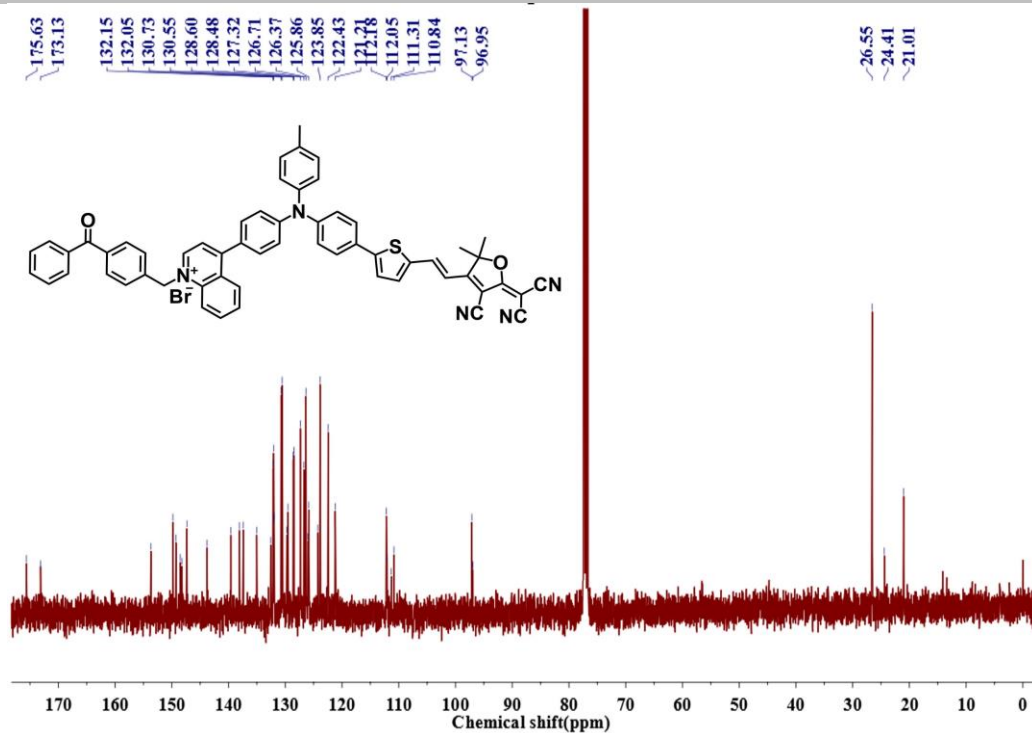


Fig. S15  $^{13}\text{C}$  NMR spectrum of FCN-TPAQ-BP in  $\text{CDCl}_3$ .

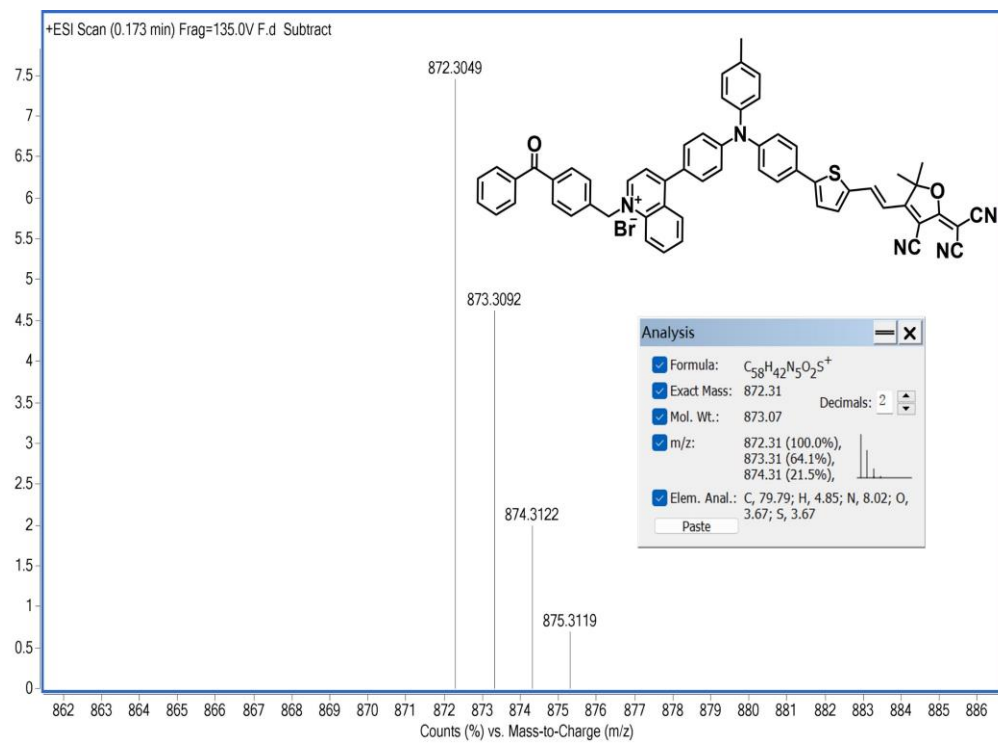


Fig. S16 ESI-MS spectrum of FCN-TPAQ-BP.

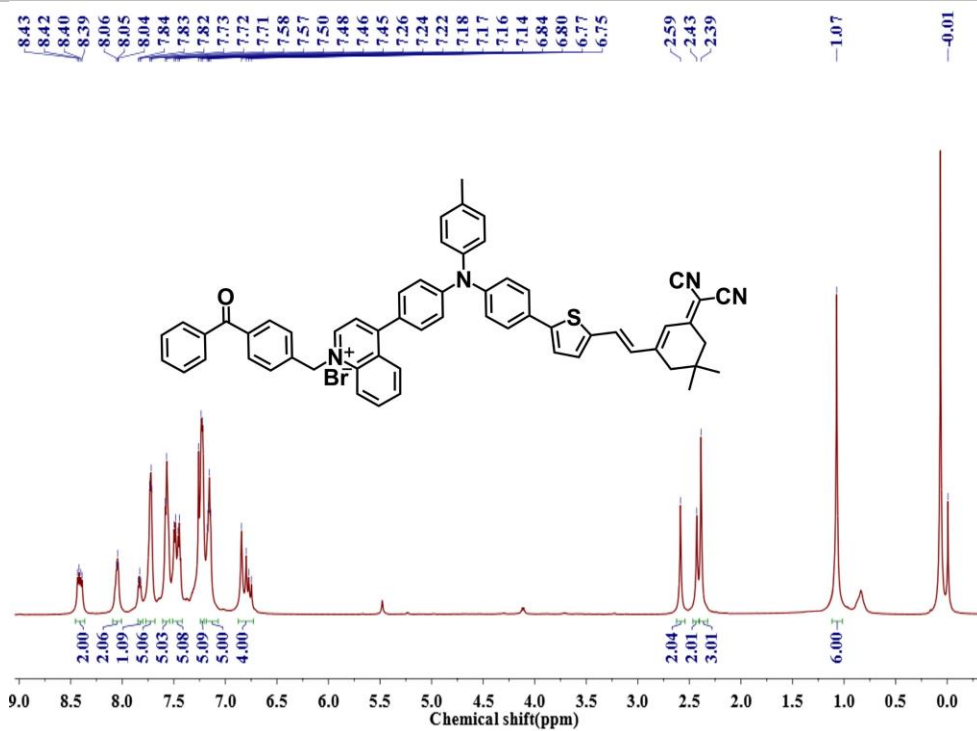


Fig. S17 <sup>1</sup>H NMR spectrum of ACN-TPAQ-BP in CDCl<sub>3</sub>.

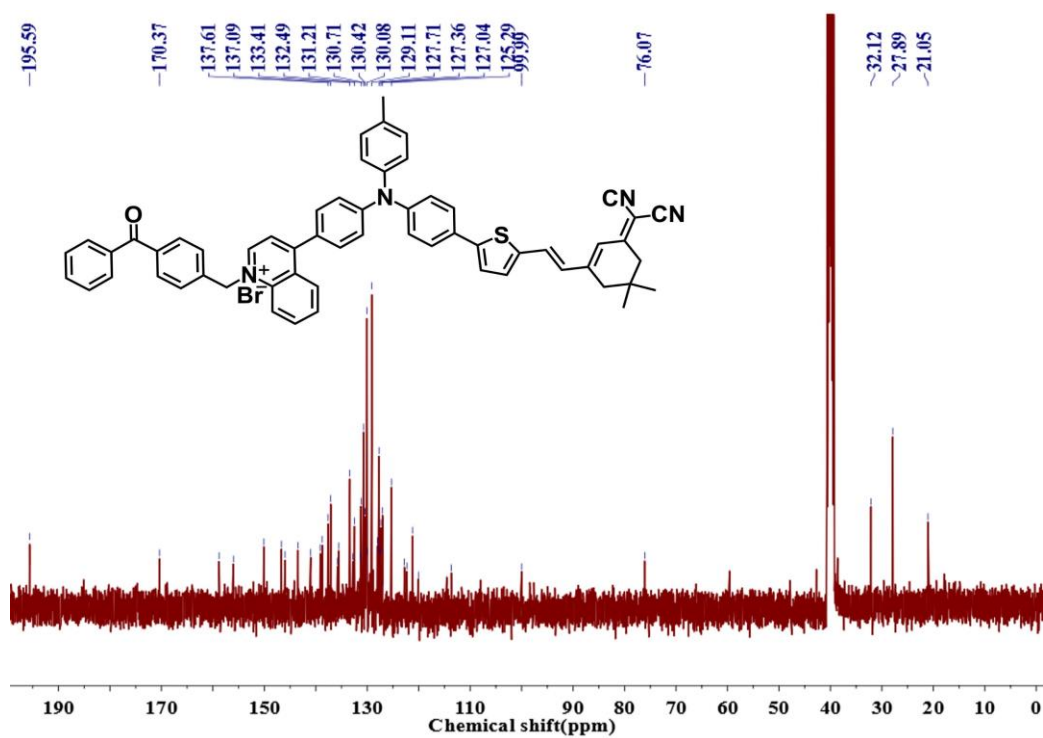
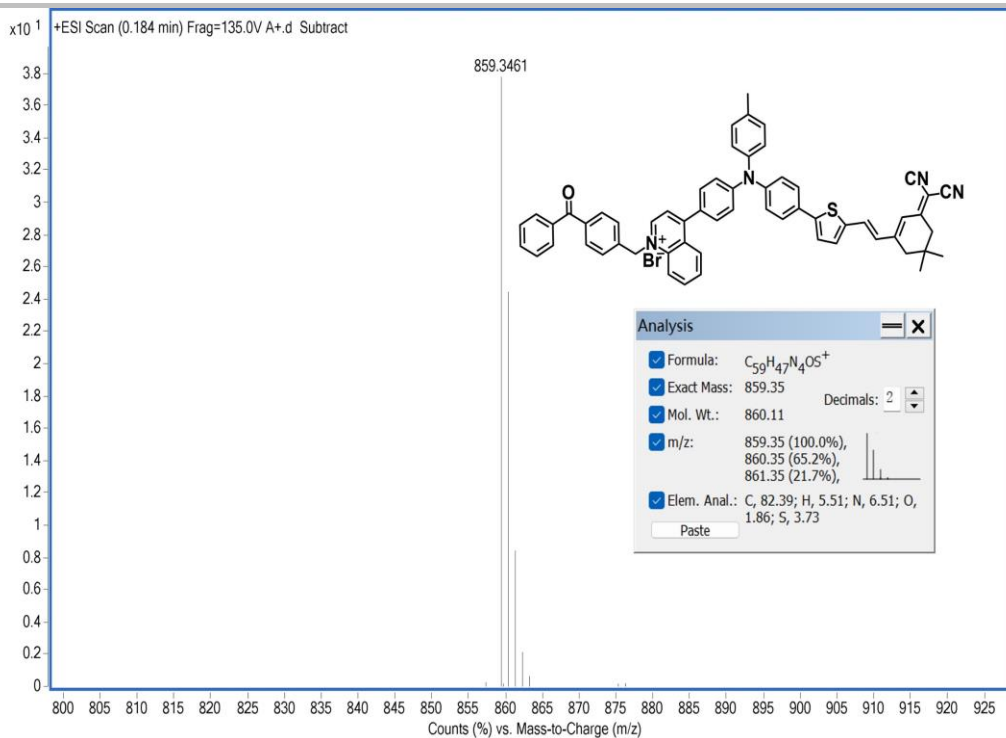


Fig. S18 <sup>13</sup>C NMR spectrum of ACN-TPAQ-BP in DMSO-*d*<sub>6</sub>.



**Fig. S19** ESI-MS spectrum of ACN-TPAQ-BP.

### 3 Results and Discussion

#### 3.1 Photophysical Properties

**Table S1.** Calculated energy of the singlet (S) and triplet (T) excited states

Compounds	CN-TPAQ-BP	ICN-TPAQ-BP	FCN-TPAQ-BP	ACN-TPAQ-BP
S <sub>1</sub>	2.6030	2.6318	2.5962	2.5189
S <sub>2</sub>	3.5918	3.1041	3.1506	3.0053
S <sub>3</sub>	3.6477	3.5519	3.3335	3.2529
T <sub>1</sub>	1.7949	1.7048	1.3726	1.3023
T <sub>2</sub>	1.9217	1.9405	1.9202	1.8553
T <sub>3</sub>	2.8313	2.3326	2.4052	2.3979
T <sub>4</sub>	3.0127	2.8672	2.8189	2.7856
T <sub>5</sub>	3.0754	3.0049	3.0125	2.9626
T <sub>6</sub>	3.3421	3.0113	3.0299	3.0098
T <sub>7</sub>	3.4155	3.1686	3.2828	3.1731

**Table S2.** Photophysical properties of the compounds

Compounds	$\lambda_{\text{abs}}$ (nm)	$\lambda_{\text{em}}$ (nm)	$\epsilon$ (M <sup>-1</sup> cm <sup>-1</sup> )	$\tau$ (ns)		ROS yield (RB=1)	$\Delta E_{\text{L-H}}$ (eV)	SOC constant (S <sub>1</sub> -T <sub>1</sub> )
				$\tau_1$	$\tau_2$			
CN-TPAQ-BP	496	806	18600	2.01	13.41	3.208	3.921	0.5630
ICN-TPAQ-BP	491	822	10400	1.87	14.32	3.493	4.128	0.450
FCN-TPAQ-BP	500	873	14800	2.10	13.49	4.760	3.928	0.6795
ACN-TPAQ-BP	500	815	21800	2.00	14.32	4.480	3.934	0.6363

#### 3.2 AIE properties

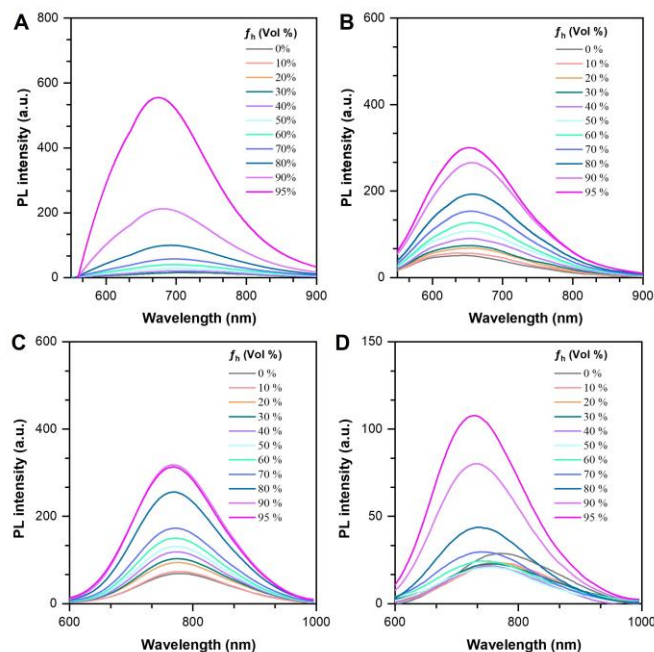


**Fig. S20** PL spectra of (A) CN-TPAQ-BP, (B) ICN-TPAQ-BP, (C) FCN-TPAQ-BP, (D) ACN-TPAQ-BP, in acetonitrile/diethyl ether mixture with different diethyl ether fractions (0-95%).

#### 3.3 Photostability and solvation effect

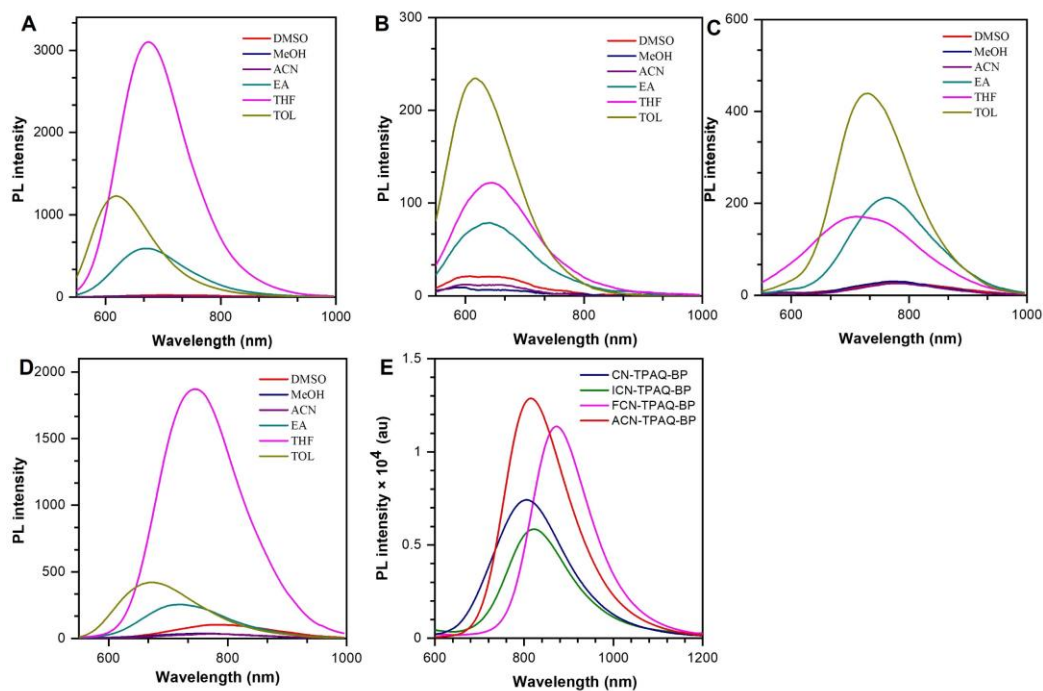


**Fig. S21** PL spectra of (A) CN-TPAQ-BP, (B) ICN-TPAQ-BP, (C) FCN-TPAQ-BP, (D) ACN-TPAQ-BP in different solvents (10  $\mu$ M). (E) PL spectra of compounds in the solid state.

### 3.4 ROS generation

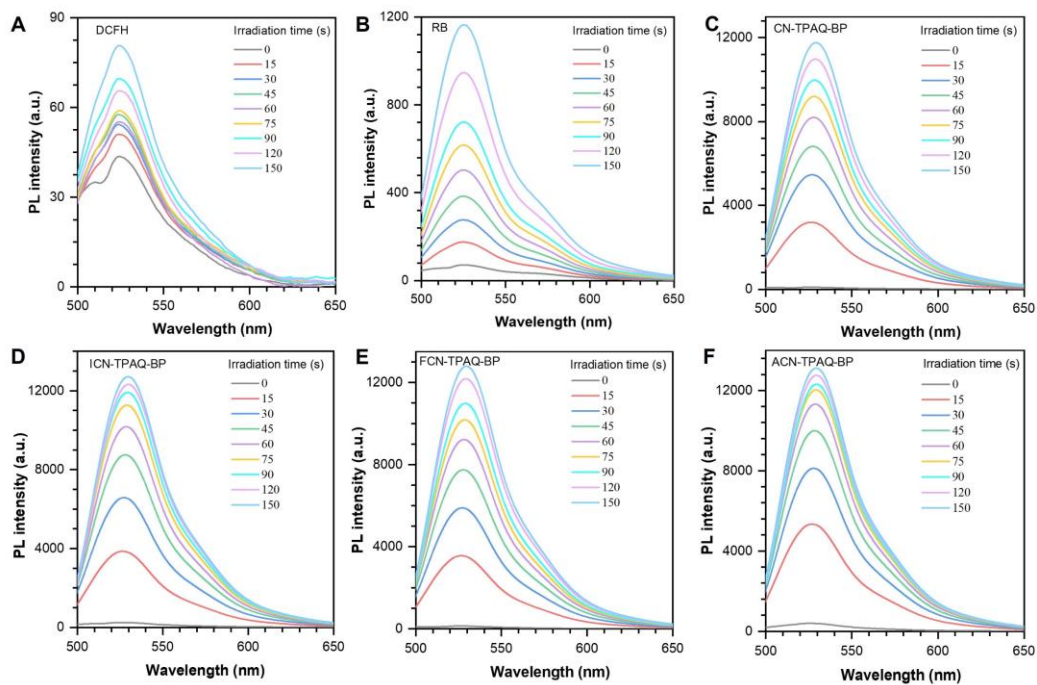


**Fig. S22** ROS generation of (A) DCFH, (B) RB, (C) CN-TPAQ-BP, (D) ICN-TPAQ-BP, (E) FCN-TPAQ-BP, and (F) ACN-TPAQ-BP (1  $\mu$ M) upon exposure to white light using DCFH (10  $\mu$ M) as an indicator.

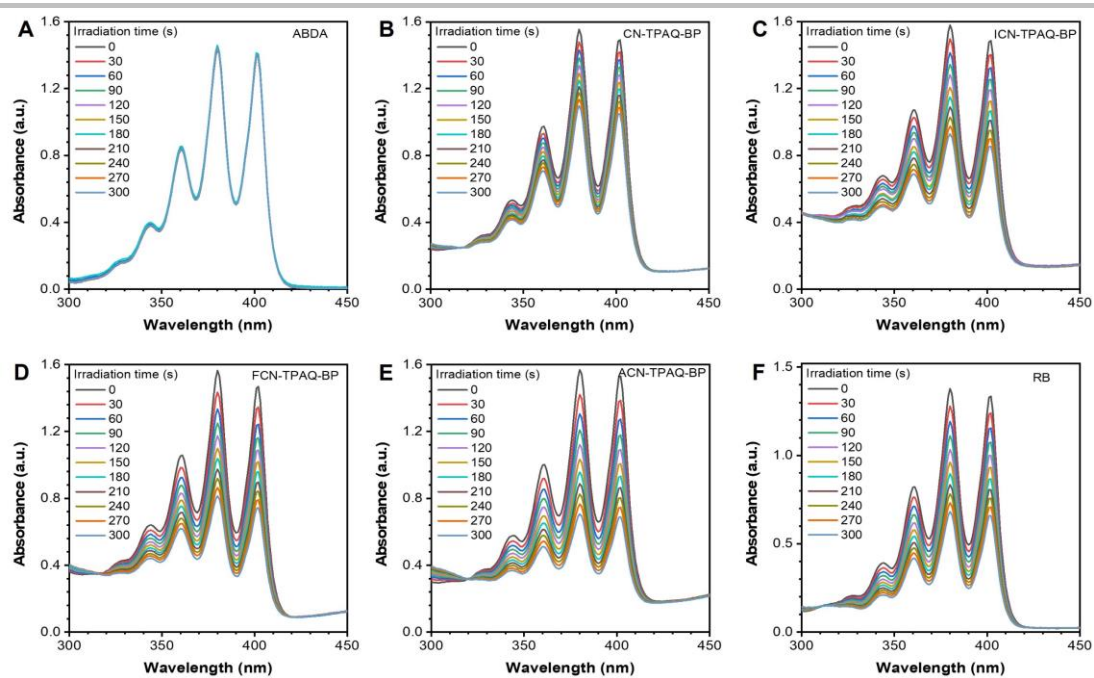


**Fig. S23** Absorption of ABDA (50  $\mu\text{M}$ ,  $^1\text{O}_2$  probe) in water in the absence (blank, A) and presence of (B) CN-TPAQ-BP, (C) ICN-TPAQ-BP, (D) FCN-TPAQ-BP, (E) ACN-TPAQ-BP and (F) RB (10  $\mu\text{M}$ ) under white light irradiation for different time.

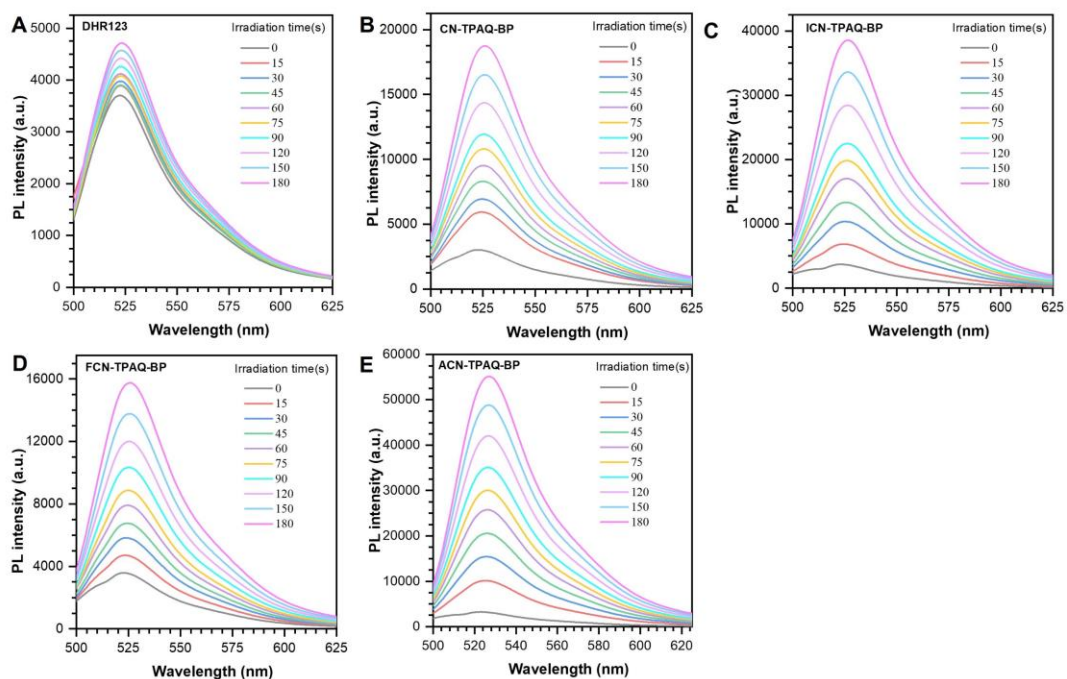


**Fig. S24** PL spectra of DHR 123 (5  $\mu\text{M}$ ) in PBS in the presence of (A) blank, (B) CN-TPAQ-BP, (C) ICN-TPAQ-BP, (D) FCN-TPAQ-BP and (E) ACN-TPAQ-BP (1  $\mu\text{M}$ ) after exposure to white light irradiation (10  $\text{mW cm}^{-2}$ ) with different time.

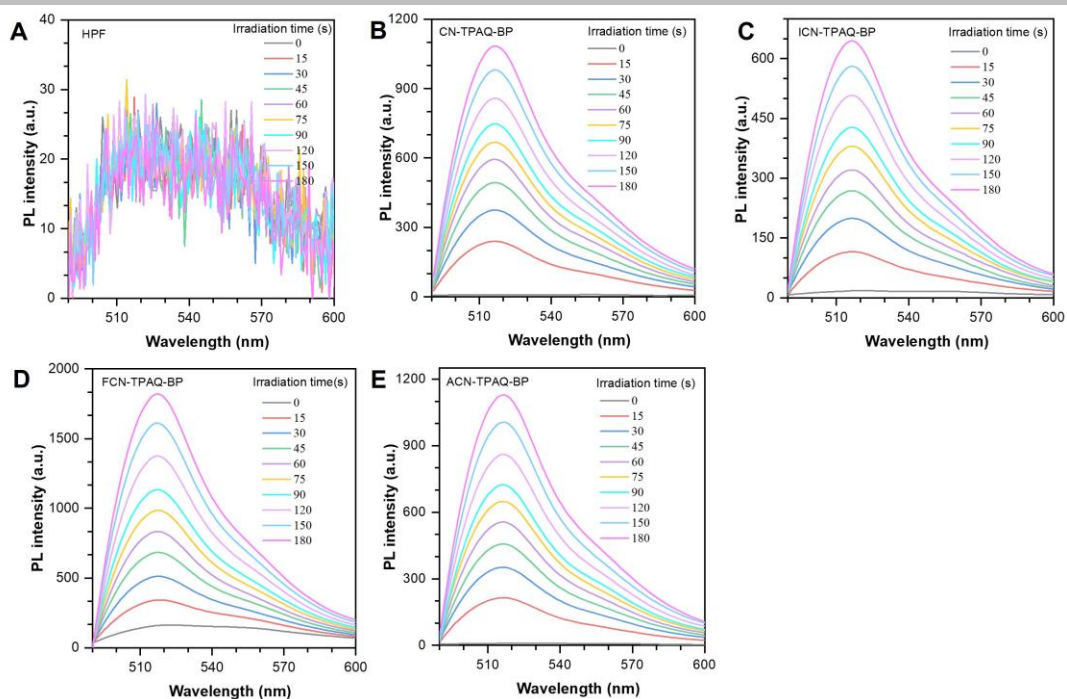


**Fig. S25** PL spectra of HPF (5  $\mu\text{M}$ ,  $\bullet\text{OH}$  probe) in the absence (blank, A) and presence of (B) CN-TPAQ-BP, (C) ICN-TPAQ-BP, (D) FCN-TPAQ-BP and (E) ACN-TPAQ-BP (1  $\mu\text{M}$ ) in PBS upon white light irradiation with 10  $\text{mW cm}^{-2}$  for different time.

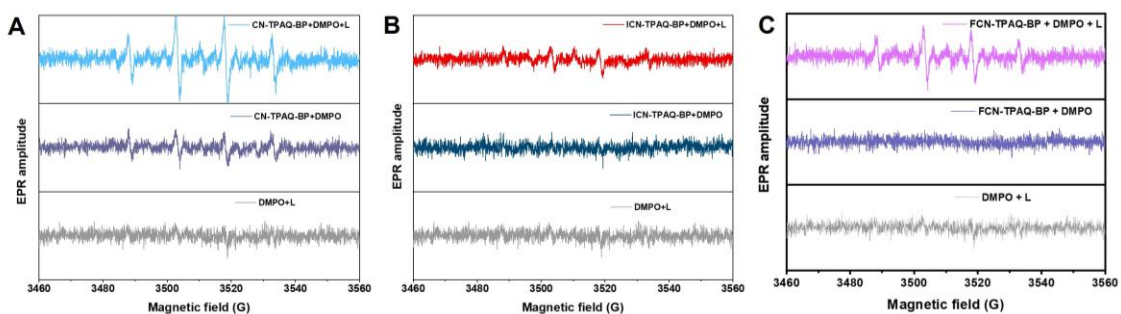


**Fig. S26** EPR signals of DMPO (10  $\mu\text{L}$ ) in the presence (A) CN-TPAQ-BP and (B) ICN-TPAQ-BP (C) FCN-TPAQ-BP in  $\text{H}_2\text{O}$  with/without white light irradiation (10  $\text{mW cm}^{-2}$ ) for 5 min.

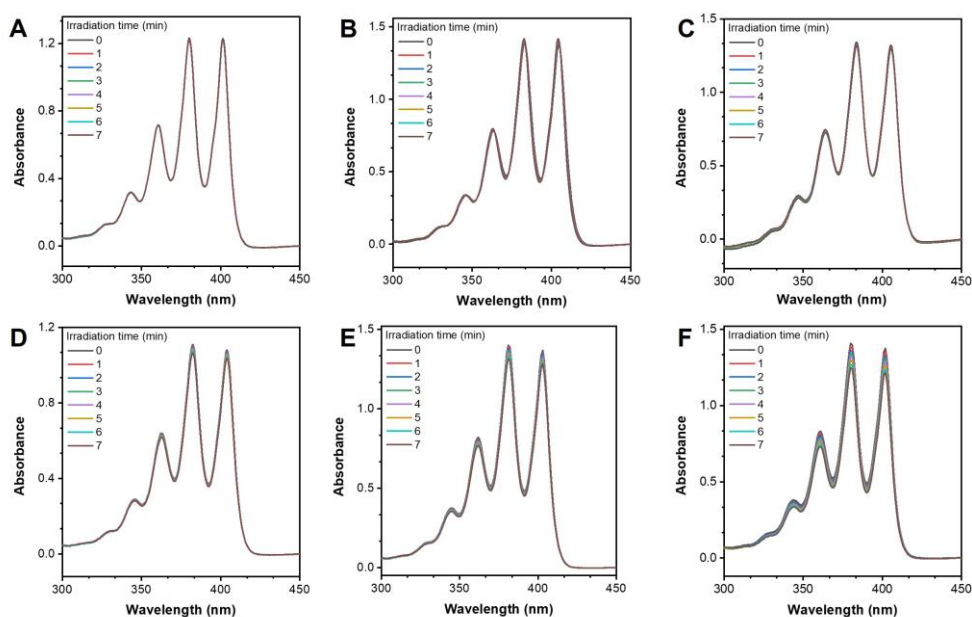




**Fig. S27** (A-F) The absorbance spectra of ABDA (100  $\mu\text{M}$ ,  $^1\text{O}_2$  probe) in the presence of CN-TPAQ-BP (10  $\mu\text{M}$ ) in mixtures of DMSO and PBS with different PBS fractions (0%, 20%, 40%, 60%, 80% and 95%) upon white-light irradiation (10  $\text{mW cm}^{-2}$ ).

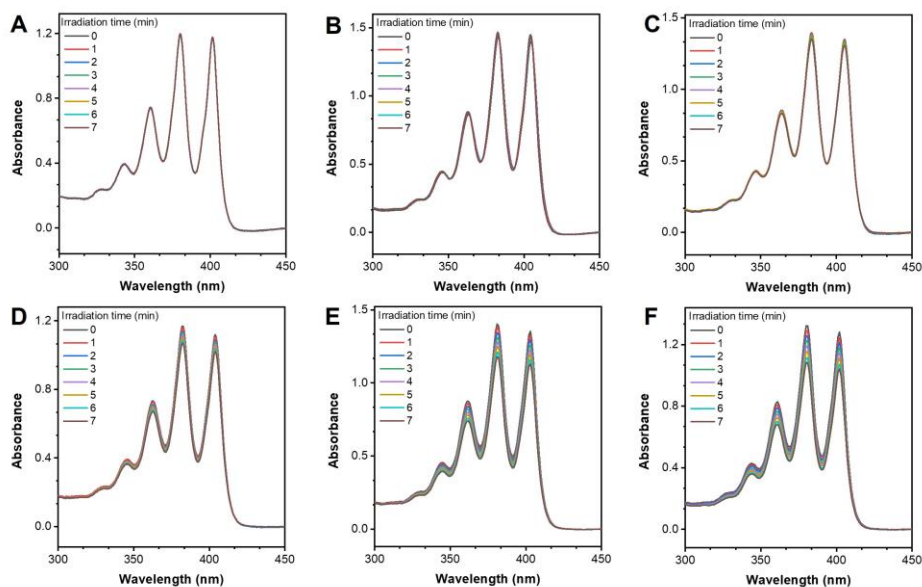


**Fig. S28** (A-F) The absorbance spectra of ABDA (100  $\mu\text{M}$ ,  $^1\text{O}_2$  probe) in the presence of ICN-TPAQ-BP (10  $\mu\text{M}$ ) in mixtures of DMSO and PBS with different PBS fractions (0%, 20%, 40%, 60%, 80% and 95%) upon white-light irradiation (10  $\text{mW cm}^{-2}$ ).

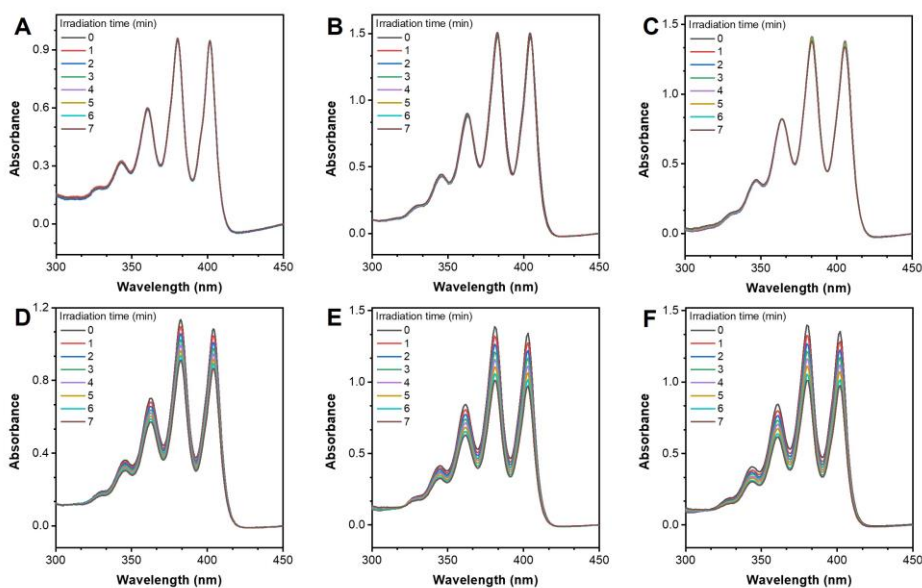


**Fig. S29** (A-F) The absorbance spectra of ABDA (100  $\mu\text{M}$ ,  $^1\text{O}_2$  probe) in the presence of FCN-TPAQ-BP (10  $\mu\text{M}$ ) in mixtures of DMSO and PBS with different PBS fractions (0%, 20%, 40%, 60%, 80% and 95%) upon white-light irradiation (10  $\text{mW cm}^{-2}$ ).

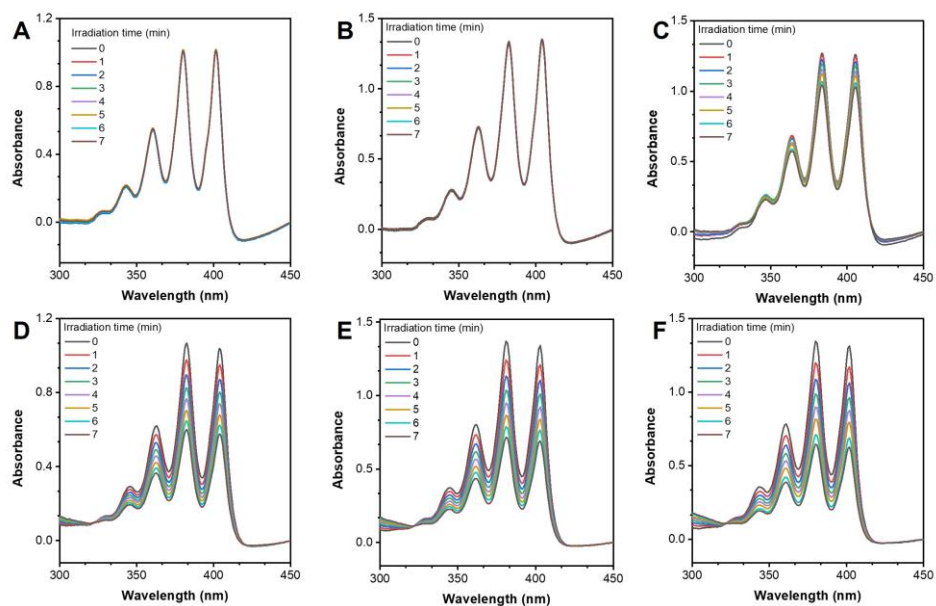


**Fig. S30** (A-F) The absorbance spectra of ABDA (100  $\mu\text{M}$ ,  $^1\text{O}_2$  probe) in the presence of ACN-TPAQ-BP (10  $\mu\text{M}$ ) in mixtures of DMSO and PBS with different PBS fractions (0%, 20%, 40%, 60%, 80% and 95%) upon white-light irradiation (10  $\text{mW cm}^{-2}$ ).

### 3.5 Cell Imaging and cell viability

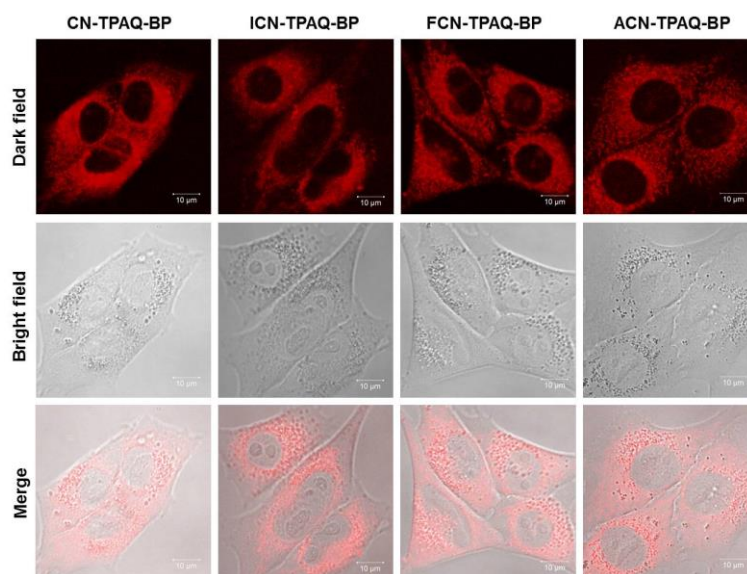


**Fig. S31** Fluorescence images of 4T1 cells stained with 10  $\mu\text{M}$  CN-TPAQ-BP, ICN-TPAQ-BP, FCN-TPAQ-BP and ACN-TPAQ-BP for 6 h, respectively.

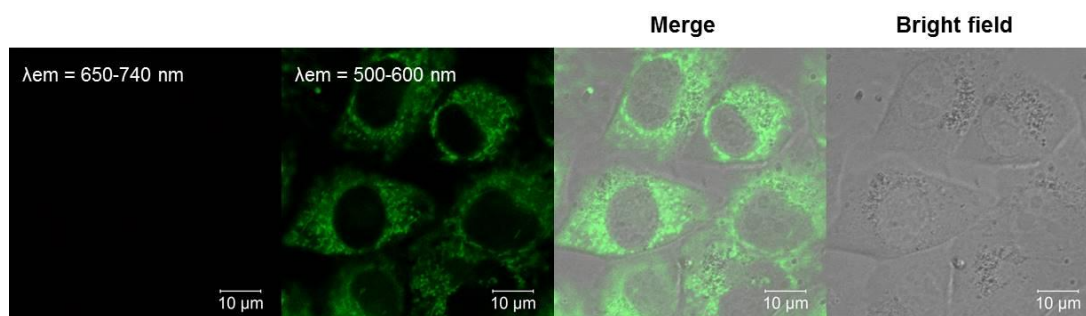


**Fig. S32** CLSM images of 4T1 cells co-stained with MitoTracker Green (conc.: 1  $\mu\text{M}$ ), incubation time: 0.5 h,  $\lambda_{\text{ex}} = 488 \text{ nm}$ ).

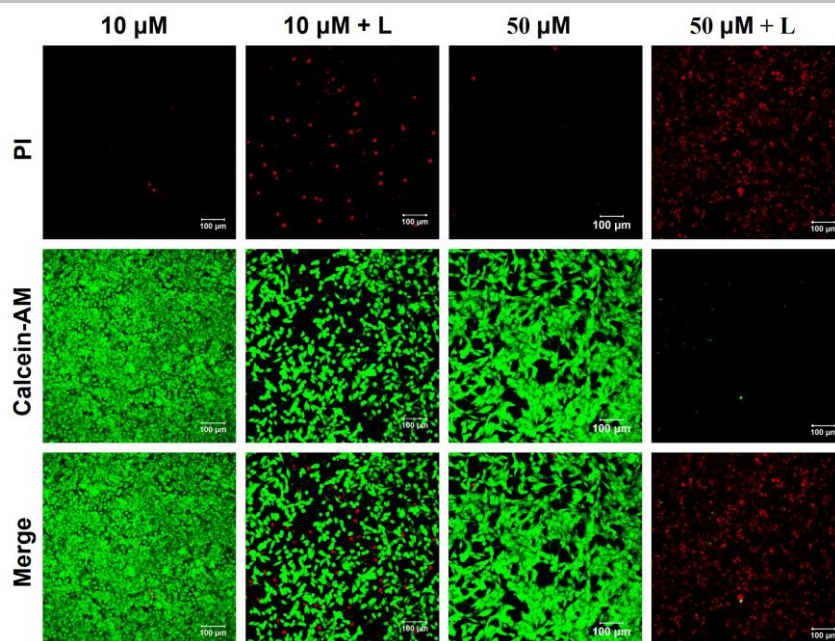


Fig. S33 Live/dead staining assay of 4T1 cells after various treatments of CN-TPAQ-BP.

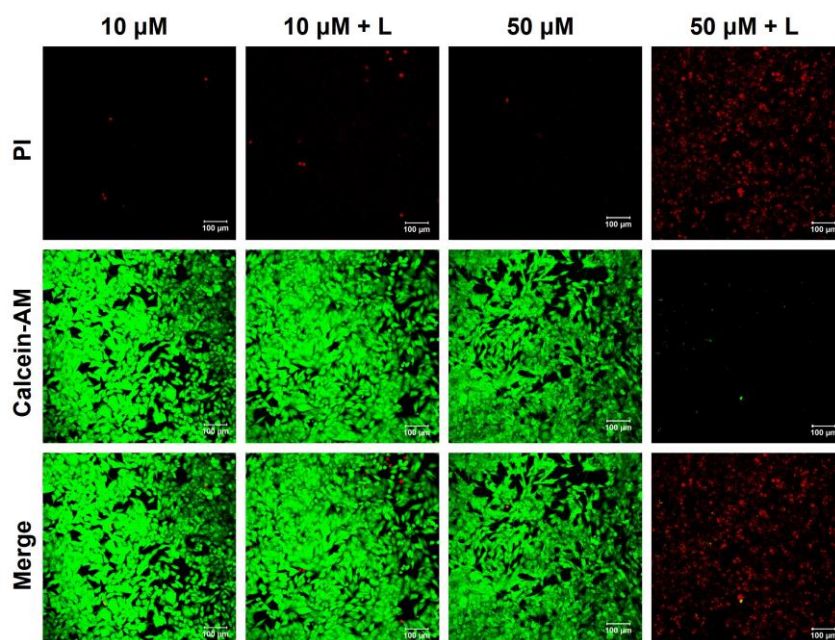
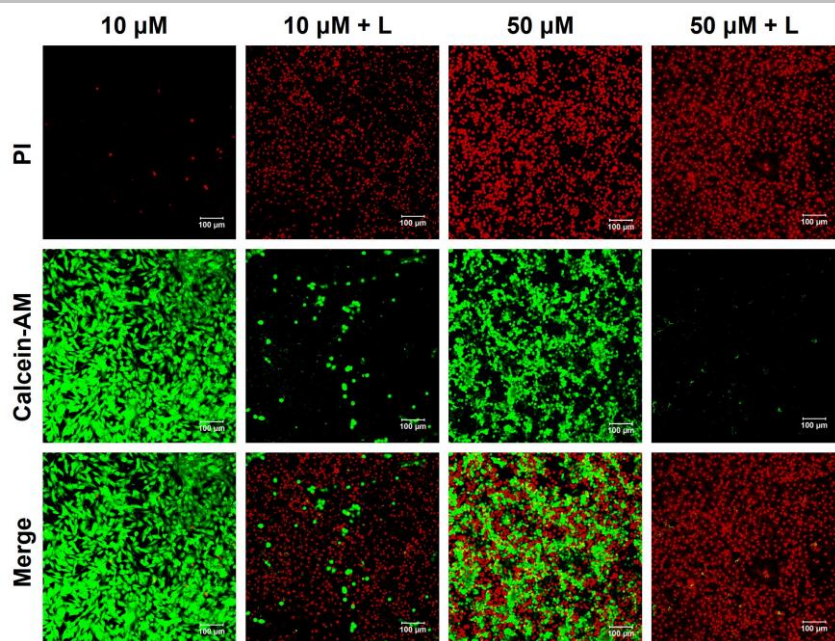
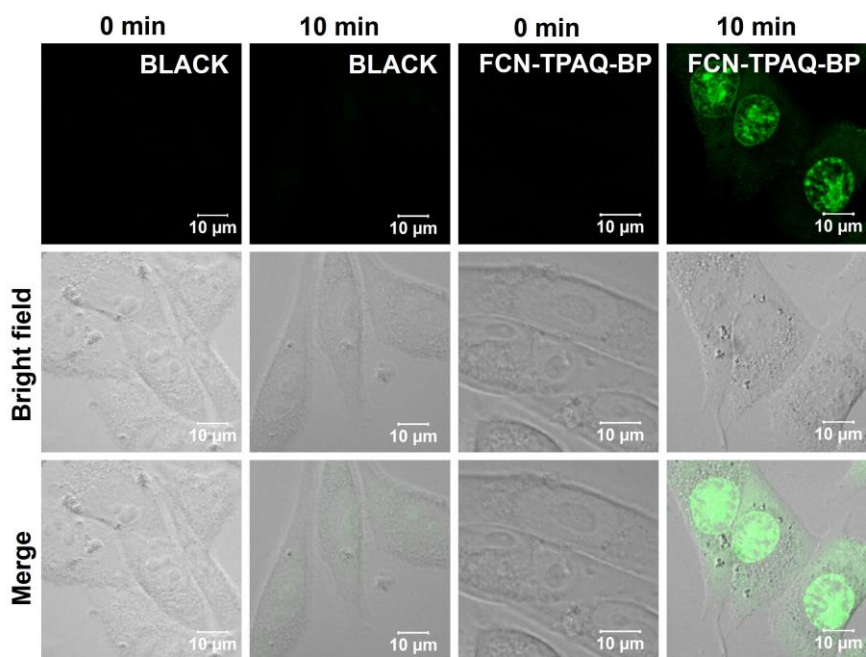


Fig. S34 Live/dead staining assay of 4T1 cells after various treatments of ICN-TPAQ-BP.



**Fig. S35** Live/dead staining assay of 4T1 cells after various treatments of ACN-TPAQ-BP.



**Fig. S36**  $\text{O}_2^{\cdot -}$  generation of FCN-TPAQ-BP (10  $\mu\text{M}$ ) in 4T1 cells by using DHE (5  $\mu\text{M}$ ) as indicators, before and after exposure to white light (0.4  $\text{mW cm}^{-2}$ ) irradiation.

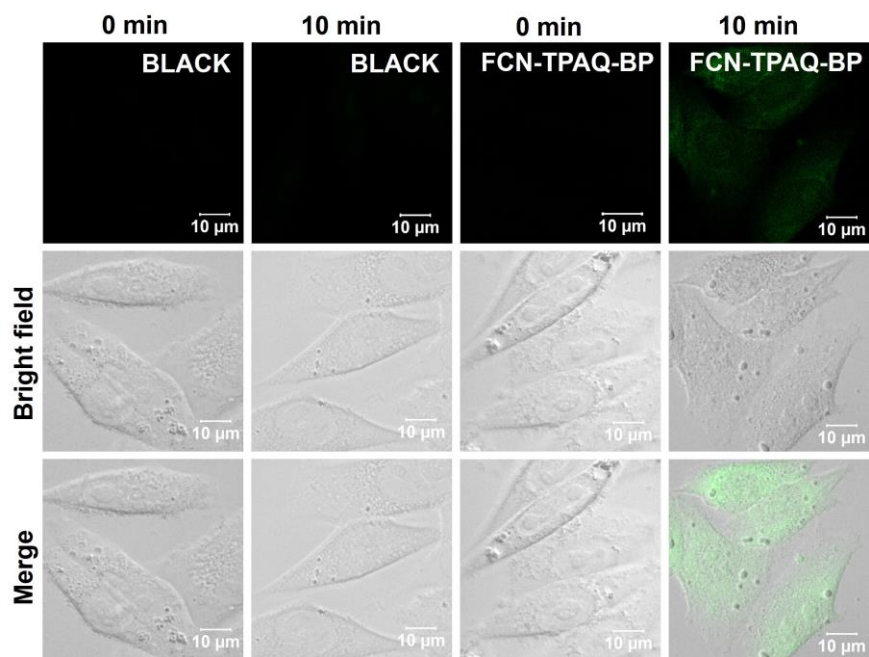


**Fig. S37** •OH generation of FCN-TPAQ-BP (10  $\mu$ M) in 4T1 cells by using HPF (5  $\mu$ M) as indicators, before and after exposure to white light (0.4 mW cm<sup>-2</sup>) irradiation.